



Gene Signatures Detect Damaged Liver Sinusoidal Endothelial Cells in Chronic Liver Diseases

Stefaan Verhulst^{**†}, Elise Anne van Os[†], Vincent De Smet, Nathalie Eysackers, Inge Mannaerts and Leo A. van Grunsven^{*}

Liver Cell Biology Research Group, Vrije Universiteit Brussel, Brussel, Belgium

OPEN ACCESS

Edited by:

Jinhang Gao,
Sichuan University, China

Reviewed by:

Kunimaro Furuta,
Mayo Clinic, United States
Jianwen Lu,
The First Affiliated Hospital of Xi'an
Jiaotong University, China

*Correspondence:

Stefaan Verhulst
stefaan.verhulst@vub.be
Leo A. van Grunsven
leo.van.grunsven@vub.be

[†]These authors share first authorship

Specialty section:

This article was submitted to
Gastroenterology,
a section of the journal
Frontiers in Medicine

Received: 30 July 2021

Accepted: 21 September 2021

Published: 20 October 2021

Citation:

Verhulst S, van Os EA, De Smet V, Eysackers N, Mannaerts I and van Grunsven LA (2021) Gene Signatures Detect Damaged Liver Sinusoidal Endothelial Cells in Chronic Liver Diseases. *Front. Med.* 8:750044. doi: 10.3389/fmed.2021.750044

Liver sinusoidal endothelial cells have a gatekeeper function in liver homeostasis by permitting substrates from the bloodstream into the space of Disse and regulating hepatic stellate cell activation status. Maintenance of LSEC's highly specialized phenotype is crucial for liver homeostasis. During liver fibrosis and cirrhosis, LSEC phenotype and functions are lost by processes known as capillarization and LSEC dysfunction. LSEC capillarization can be demonstrated by the loss of fenestrae (cytoplasmic pores) and the manifestation of a basement membrane. Currently, no protein or genetic markers can clearly distinguish healthy from damaged LSECs in acute or chronic liver disease. Single cell (sc)RNA sequencing efforts have identified several LSEC populations in mouse models for liver disease and in human cirrhotic livers. Still, there are no clearly defined genesets that can identify LSECs or dysfunctional LSEC populations in transcriptome data. Here, we developed genesets that are enriched in healthy and damaged LSECs which correlated very strongly with healthy and early stage- vs. advanced human liver diseases. A damaged LSEC signature comprised of *Fabp4/5* and *Vwf/a1* was established which could efficiently identify damaged endothelial cells in single cell RNAseq data sets. In LSECs from an acute CCl₄ liver injury mouse model, *Fabp4/5* and *Vwf/a1* expression is induced within 1–3 days while in cirrhotic human livers these 4 genes are highly enriched in damaged LSECs. In conclusion, our newly developed gene signature of damaged LSECs can be applicable to a wide range of liver disease etiologies, implicating a common transcriptional alteration mechanism in LSEC damage.

Keywords: LSEC, acute liver injury, single cell RNA sequencing (scRNAseq), primary cells, NAFLD (non-alcoholic fatty liver disease), non-alcoholic steatohepatitis (NASH)

INTRODUCTION

Liver sinusoidal endothelial cells (LSECs) comprise about 15–20% of the total number of liver cells and line the sinusoidal lumen of the liver sinusoids. LSECs are highly specialized endothelial cells characterized by fenestrae and lack of a basement membrane (1) making these cells the most permeable cells in the mammalian body (2). LSEC permeability is important for liver function as it permits plasma, solutes, and small substrates such as albumin (3) and insulin (4) to diffuse from the blood toward the parenchymal cells. Besides working as a filter and first barrier of the liver, these cells have other functions such as the production of coagulation factor VIII (5), antigen presentation (6, 7), leukocyte recruitment and endocytosis of virus particles (8), oxidized

LDL (9) and immunocomplexes by the abundant expression of multiple scavenger receptors (10). Expression of specific scavenger receptors and other characteristic proteins can vary across the liver acinus (11, 12).

Maintenance of the specialized LSEC phenotype is essential for liver homeostasis (13). During liver injury LSECs can become dysfunctional, characterized by the loss of fenestrae and the appearance of a basement membrane, also known as capillarization (4, 14–16). LSECs can contribute to liver regeneration and healing by orchestrating an angiocrine response that can lead to a pro-regenerative response after an acute injury or to a maladaptive pro-fibrotic response after chronic injury, which in turn leads to fibrosis (17). Moreover, LSECs are described to have a gatekeeper function in liver fibrosis as differentiated LSECs promote HSC quiescence, and restoration of LSEC differentiation can prevent fibrosis progression and accelerate fibrosis regression (18). Although it is known that LSECs play an important role in the response to acute and chronic liver injury, research on the transcriptomic and phenotypic change of LSECs during acute and chronic injury is still limited. In addition, identification of LSECs using genetic/protein markers is still quite controversial (19) as there is no unique marker that characterizes LSECs (11, 13) apart from fenestrae and the absence of a basement membrane. The identification of damaged LSECs in an acute or chronic setting is even more challenging. Recently, specific markers for LSECs in healthy livers have been described, such as CD32b (20), CLEC4G (21), LYVE1 (22), STAB2 (23) in addition to the more controversial endothelial cell (EC) markers VWF and CD31 which are upregulated in LSECs during disease (13, 19). However, currently electron microscopy is still the golden standard for identification of damaged LSECs (loss of fenestrae). The recent use of single-cell transcriptomics (scRNAseq), performed on both healthy and diseased human and mouse livers, has identified several heterogeneous hepatic cell populations, including LSECs (12, 21, 24–26). These publicly available data sets present bioinformatic opportunities to define LSEC populations more efficiently in both healthy and diseased livers, independent of the etiology or background.

In this study, we developed healthy- and damaged LSEC enriched gene sets and signatures using healthy and cirrhotic human liver scRNAseq data and newly generated datasets from healthy and acutely injured mouse livers. These LSEC genesets and signatures can identify the health status of LSECs in mouse and human bulk transcriptome or scRNAseq data from chronic or acute liver diseases. Using these gene sets, we demonstrate that LSECs are dysfunctional in multiple end-stage liver diseases and that LSECs are quickly damaged upon an acute liver injury. These results highlight the important role of LSECs in liver pathophysiology.

MATERIALS AND METHODS

Animals

All methods and protocols were carried out according to the approved guidelines of the Vrije Universiteit Brussel (VUB, Belgium) and according to European Guidelines for the Care and

Use of Laboratory Animals. Animal experiment protocols were approved by the Ethical Committee of Animal Experimentation of the Vrije Universiteit Brussel (VUB, Belgium, 14-212-4). BalbC mice aged 11–14 weeks were housed in a controlled environment in conventional cages and were allowed food and water *ad libitum*. Acute liver injury in BalbC mice was induced by a single intraperitoneal injection with 15 μ l carbon tetrachloride (CCl₄, 87031, Sigma-Aldrich, St. Louis, MO, USA) and 85 μ l mineral oil (Sigma-Aldrich, St. Louis, MO, USA) per 30 g bodyweight. Blood, total liver and cells were collected from healthy mice and after 1, 3 and 7 days of CCl₄ administration. Mice were anesthetized using 100 μ L Dolethal[®] (Vetoquinol, France). Analysis of alanine aminotransferase (ALT) was performed using a SPOTCHEM EZ SP-4430 (A.Menarini Diagnostics, The Netherlands). At the start and end of the experiment mice were weighted. Daily observation of the mice showed only a mild effect on animal welfare.

LSEC Isolation From Mice

Non-parenchymal cells (NPCs) were retrieved as previously described (27). Red blood cell lysis (Miltenyi Biotec, Germany) was performed, and NPCs were washed with PBS + 0.1% Bovine Serum Albumin (BSA). NPCs were resuspended in BPE buffer (PBS with 5% BSA and 2 mM EDTA) with 1 μ l anti-mouse Fc block[™] (Becton-Dickinson, Belgium) reagent added per 10⁷ cells for 10 min at 4°C. Cells were washed and incubated in 600 μ L PBS+0.1% BSA with 5 μ l CD32-PE (ab30357, Abcam, UK), 2 μ L CD45-FITC (11-0451-85, eBioscience, USA) and 10 μ l F4/80 Alexa-647 per 10⁷ cells (MF48021, Life Technologies) for 15 min at 4°C. After incubation with the antibodies, cells were washed and resuspended in a buffer solution without calcium and supplemented with DNase I (3:1, 10104159001, Roche, Switzerland) before cell isolation using FACS (FACS Aria IIu, BD Biosciences, Belgium). FACS was used to sort viable cells (negative selection based on propidium iodide) and LSECs were selected and sorted based on a positive signal for CD32 (27–29) and a negative signal for UV, F4/80, CD45. CD32b is expressed in all LSECs across the liver sinusoid (**Supplementary Figure 1A**) (30). Potential doublets with HSCs, KCs, and immune cells were excluded (cfr. **Supplementary Figure 1B**. Utmost right FACS plot with circled LSEC population). Stainings were performed on cytopins after isolation and showed a high purity (95%) of LSECs using this sorting strategy (**Supplementary Figure 1C**).

RNA Preparation and Sequencing

Total RNA was extracted from FACS-isolated LSECs using ReliaPrep RNA Cell Miniprep System (Z6012, Promega, USA), RNA concentrations and quality measurements were performed using a Bioanalyzer 6000. Preparation of samples and sequencing, using Clontech SMARTseq v4 kit (R400752, Takara, Japan) and NovaSeq S2 (2 \times 100 bp), was performed by the BRIGHTcore of the Vrije Universiteit Brussel. Single-end sequencing was run on Illumina NextSeq 500 High.

Immunofluorescence

Mouse liver tissues were fixed with formalin for 48 h at 4°C. Liver tissues were stored in 70% EtOH and were used for sectioning (Leica, The Netherlands) of 100 μ m liver sections

in 4% UltraPure™ Low Melting Point Agarose (Invitrogen, USA) using a vibratome (Leica, The Netherlands). Sections were kept in 70% EtOH until usage. Upon usage sections were rehydrated in 50% EtOH for 10 min and rinsed for 10 min with PBS. For permeabilization, sections were incubated with PBS + 0.2% Triton for 20 min at room temperature. After permeabilization, sections were washed two times with PBS and blocked with 3% BSA-PBS for 2 h at room temperature. Sections were incubated overnight at room temperature with the following primary antibodies; Lyve1 (2 µg/mL, AF2125, R&D systems, Canada), Ki67 (0.5 µg/mL, 14-5698-82, Thermofisher, USA) and CD32b (10 mg/mL, AF2125, R&D systems, Canada). PHEM buffer (10 mM PIPES, 25 mM HEPES, 10 mM EGTA, 2 mM MgCl₂*6H₂O) was used for CD32b staining instead of PBS in all steps. Vibratome sections were washed three times with PBS for 10 min and were incubated for 1 h with the following secondary antibodies (1:200); Donkey-anti-goat Alexa488 (A11055, Thermofisher, USA) and Donkey-anti-rat Alexa 647 (ab150155, Abcam, UK). Sections were washed three times with PBS, incubated for 10 min with 70% EtOH and then incubated with 1% Sudan Black (199664, Sigma-Aldrich, Belgium) in 70% EtOH. Sections were rinsed with PBS and mounted with Mowiol (9002-89-5, Sigma-Aldrich, Belgium) with DAPI (D9564, 10 µg/mL, Sigma-Aldrich, Belgium) and visualized by EVOS M7000 (Thermofischer, USA) and Zeiss Axioscan (Zeiss, Germany). Quantification was performed with HALO 3.1 image analysis platform (Indica labs Inc., USA).

Immunohistochemistry

Liver tissues were embedded in paraffin, sliced in 5 µm sections and deparaffinized with Xylene. For H&E stainings sections were rehydrated, washed with PBS and counterstained with Harris Hematoxylin (1:10 Roth, Newport Beach, CA, USA) before being rinsed with acid water followed by 10 min wash with tap water. Sections were incubated with eosin for 5 min, shortly rinsed, dehydrated and mounted with DPX mounting medium (Sigma-Aldrich, Belgium). For Collagen 4 staining, sections were rehydrated, washed with PBS-0.05% Tween (PBST) and endogenous peroxidase was quenched with 3% H₂O₂ in methanol. Samples were washed three times with PBST for 5 min and incubated with 2% BSA-PBS for 1 h at room temperature. Col4 antibody (2 µg/ml, ab6586, Abcam, UK) was dissolved in 1% BSA-PBS and incubated overnight at 4°C. Sections were washed and incubated with Dako EnVision+ System- HRP Labeled Poly (K4003, Dako, Denmark) for 30 min at room temperature. Sections were washed with PBST, incubated with DAB substrate for 3 min at room temperature. Finally, samples were rinsed, counterstained with Harris Hematoxylin (1:10) and mounted with DPX mounting medium (Sigma-Aldrich, Belgium) and imaged visualized with Leica Aperio CS2 (Leica, The Netherlands). Quantification was performed with Orbit image analysis (31).

Bioinformatics scRNAseq Analysis

Raw counts of scRNAseq data from healthy and diseased livers of Ramachandran et al. (GSE136103) (25), MacParland

et al. (GSE115469) (24), Aizarani (GSE124395) (21), Xiong et al. (GSE129516) (26), and Terkelsen et al. (GSE145086) (32) was downloaded from GEO-NCBI database and imported into RStudio (<https://www.rstudio.com>). General scRNAseq analysis for quality controls, normalization, clustering and multidimensional reduction was performed using the default pipeline of R package Seurat (33). Identification of different cell clusters was performed using markers from the original publications and visualized in a UMAP plot.

Differential Expressed Genes in scRNAseq Data

Genes differentially expressed between two populations were identified using the *findmarker* function within R package Seurat with fold changes larger than 2.

Downstream Analysis for scRNAseq

Creation and visualization of different gene signatures (LSEC signatures) by upset plots was performed by the usage of R packaged UpSetR. Gene ontology analysis based on biological processes was analyzed using R package clusterProfiler for all gene signatures. The *AddmoduleScore* function in Seurat (version 4) was used to quantify gene signature scores of all LSEC signatures for each cell population. The gene signature score represents the average expression of all genes of the healthy or damaged LSEC gene signature within a cell population subtracted by the average expression of randomly selected genes within the same population.

Whole Transcriptome Analysis

Paired-end sequencing on RNA of LSECs isolated using FACS from healthy and CCl₄ treated mice generated a fastq file for each sample. A quality control was performed before and after trimming using FastQC (www.bioinformatics.babraham.ac.uk/projects/fastqc) and AfterQC (34) followed by mapping all reads using STAR (35) to the mouse genome GRCh38.p6. Assembly was performed on every hit using StringTie and further analyzed by R package DESeq2 (36) for normalization and statistical analysis. Principle component analysis was performed using basic R functions and visualized by R package ggplot2. The expression of a selection of genes was validated using qPCR (**Supplementary Figure 2A**). qPCR was performed as previously described (27) and primers used for qPCR are displayed in **Supplementary Figure 2B**. For microarray data, CEL files were imported using R packages oligo (37) or affy (38) and normalized by Robust Multichip Average (RMA) algorithm.

Gene Set Enrichment Analysis (GSEA)

GSEA Subramanian et al. (39) was performed on normalized counts using molecular signature databases Reactome, Biocarta and KEGG pathways. GSEA for bulk seq of LSECs was performed by comparing all groups (LSECs isolated from mouse livers after 1, 3, and 7 days CCl₄ injection) to LSECs from healthy mouse livers. All enriched pathways with a NES (normalized enrichment score) higher than 1 or lower than -1 with FDR lower than 0.25 were imported in Cytoscape and transformed into a network using EnrichmentMap (40). Pathways clustered together were named manually, based on overlapping functions, following the

protocol of Reimand et al. (41). Pathway clusters that change over time were manually summarized into a hypothetical graph created in Illustrator, based on the number of pathways within a cluster and changes after CCl₄ injection. GSEA using LSEC enriched gene sets was performed on normalized counts of healthy and liver diseases or on LSECs isolated from healthy or CCl₄ recovered livers. Following comparisons were performed to analyse LSEC signatures in advanced diseased livers vs. control groups: Hepatitis B (HBV) F3-4 vs. HBV F0-1 (GSE84044) (42), non-alcoholic steatohepatitis (NASH) F3-F4 vs. F0-F1 (GSE49541) (43), alcoholic steatohepatitis (ASH) vs. alcoholic steatosis liver (GSE103580) (44), advanced cirrhosis vs. healthy (GSE6764) (45), advanced hepatocellular carcinoma (HCC) vs. normal tissue (GSE6764) (45).

Data Availability

Bulk RNAseq data of isolated LSECs after CCl₄ treatment has been deposited in the GEO public data base under accession number: GSE180366.

Statistics

One-tailed Kruskal Wallis with Dunnett's multiple comparisons test was applied for the statics of ALT measurements, CD32b, Lyve1 and Lyve1/Ki67 stainings. Calculations were made using GraphPad Prism 9. Ns > 0.05, *P ≤ 0.05, **P ≤ 0.01.

RESULTS

Enriched Genes in LSECs From Healthy and Cirrhotic Livers Identify LSECs in Advanced Cirrhotic Liver Diseases

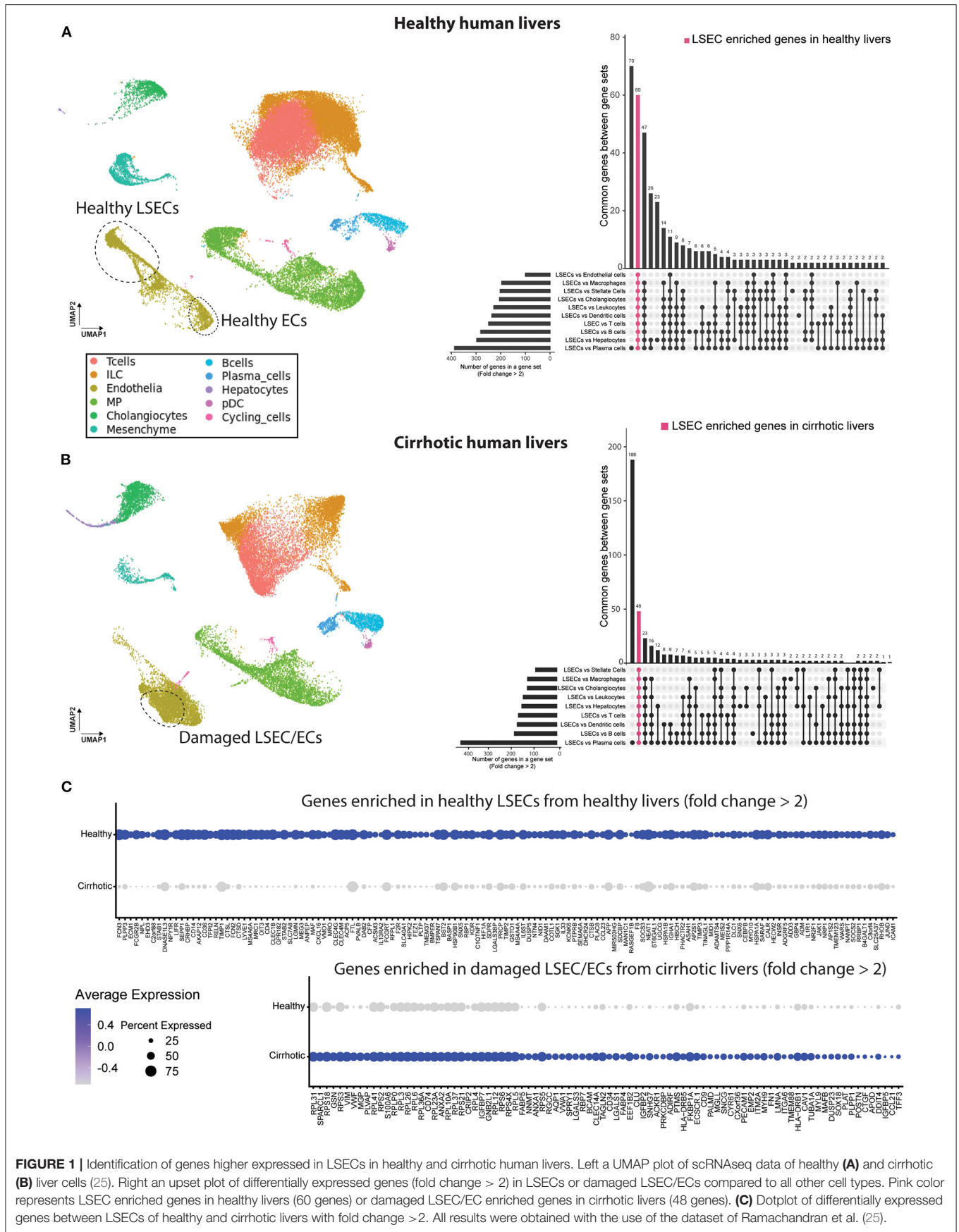
To identify the presence of healthy or dysfunctional LSECs in RNA profiling data sets from human or mouse livers we set out to identify genes that are enriched in LSECs from healthy or cirrhotic livers. To this end, we used scRNAseq data of healthy and cirrhotic human livers reported by Ramachandran et al. (25). First, we identified LSECs and ECs expressing known LSEC and EC markers in healthy livers (**Figure 1A**; **Supplementary Figure 3**). Next, we identified an additional cell population which was not present in the endothelial cell population of healthy livers (**Figure 1B**). These cells were CD34⁺PLVAP⁺VWA1⁺ positive which strongly resembled the scar-associated endothelial cell population identified by Ramachandran et al. (25). These cells were restricted to cirrhotic livers, expressed pro-fibrogenic genes and displayed an immunomodulatory phenotype (25). We refer to this population as damaged LSEC/ECs (**Figure 1B**) as some of the markers expressed in this population show a sinusoidal expression pattern in cirrhotic livers (25) but damaged ECs cannot be excluded. Subsequently, we defined genes that were higher expressed in healthy LSECs or damaged LSEC/EC population compared to all other liver cells (endothelial cells, macrophages, stellate cells, cholangiocytes, innate lymphoid cells (ILC), dendritic cells, T and B cells, hepatocytes and plasma cells) from healthy and cirrhotic livers with a fold change of at least two, and every gene should be expressed in at least 50% of cells within the healthy LSEC or damaged LSEC/EC population. This resulted in, respectively, 60

and 48 genes that were higher expressed in LSECs from healthy- or cirrhotic human livers in comparison to other liver cell types (**Figures 1A,B**). To identify genes that can further distinguish LSECs from healthy or diseased livers, we performed differential expression analysis between both populations resulting in a list of genes expressed higher in healthy LSECs compared to damaged LSEC/ECs from cirrhotic livers (**Figure 1C**). By combining genes that are enriched in LSECs from healthy or cirrhotic livers vs. other cells with genes that are higher expressed in one of the conditions vs. the other, we could create two genesets: a geneset for LSECs from healthy livers ($n = 48$) and a geneset for damaged LSEC/EC from cirrhotic livers ($n = 15$) (**Figure 2A**; **Supplementary Table 1**). Next, we performed gene ontology analyses to summarize the overlap in biological functions of genes included in each geneset. Genes that were enriched in healthy LSECs were part of GOs that are related to scavenging function and viral entry, both important characteristics of LSECs (46, 47). Genes that are enriched in damaged LSEC/EC belong to GOs that are related to dysfunctional LSECs, such as vascular development, migration and matrix organization, which are typical features of liver fibrosis (48, 49) (**Figure 2B**).

Next, we wondered whether we could use these gene sets to visualize an enrichment of damaged LSECs/ECs in microarray gene expression data from human livers. We therefore performed gene set enrichment analysis (39, 50) (GSEA) with the two LSEC gene sets on microarray gene expression data from human livers with different etiologies to identify the presence of healthy or damaged LSECs/ECs in advanced cirrhotic liver diseases. **Figure 2C** shows that gene sets that were highly expressed in healthy LSECs were substantially enriched in transcriptomes of healthy livers and diseased livers with early stage liver fibrosis (F0-F1). Gene sets that were highly expressed in damaged LSEC/ECs were enriched in cirrhotic livers (vs healthy livers) (45); ASH (vs alcoholic steatosis) (44), HCC (vs normal tissue) (45), NASH (F4-F3 vs. F0-F1) (43) and HBV (F3-4 vs. F0-1) (42) (**Figure 2D**). Taken together, our analysis suggests that LSECs transform into a more damaged endothelial cell phenotype in all advanced liver diseases that we investigated.

Dynamic Response of LSECs to CCl₄-Induced Acute Liver Injury

LSECs play a crucial role in the regenerative response after an acute injury that can either lead to liver regenerative or a maladaptive fibrotic response (17). Yet, all studies and datasets we have used so far only reflected chronic liver injury. Therefore, we wanted to know whether the gene sets could also demonstrate LSEC phenotype changes after an acute injury. To this end, acute liver injury in mice was induced with a single dose of CCl₄ and livers were collected at 1, 3, and 7 days after injection (**Figure 3A**). Blood analysis shows acute liver injury (high ALT levels) at 24h after a single dose of CCl₄, which decreases to baseline levels at day 7 (**Figure 3B**). Hematoxylin eosin staining shows necrotic areas that appear at 1 day and are more pronounced after 3 days demonstrating that liver injury is still present at that time point (**Figure 3C**). However, after 1 week the liver appears to have recovered from the injury. When we further examine



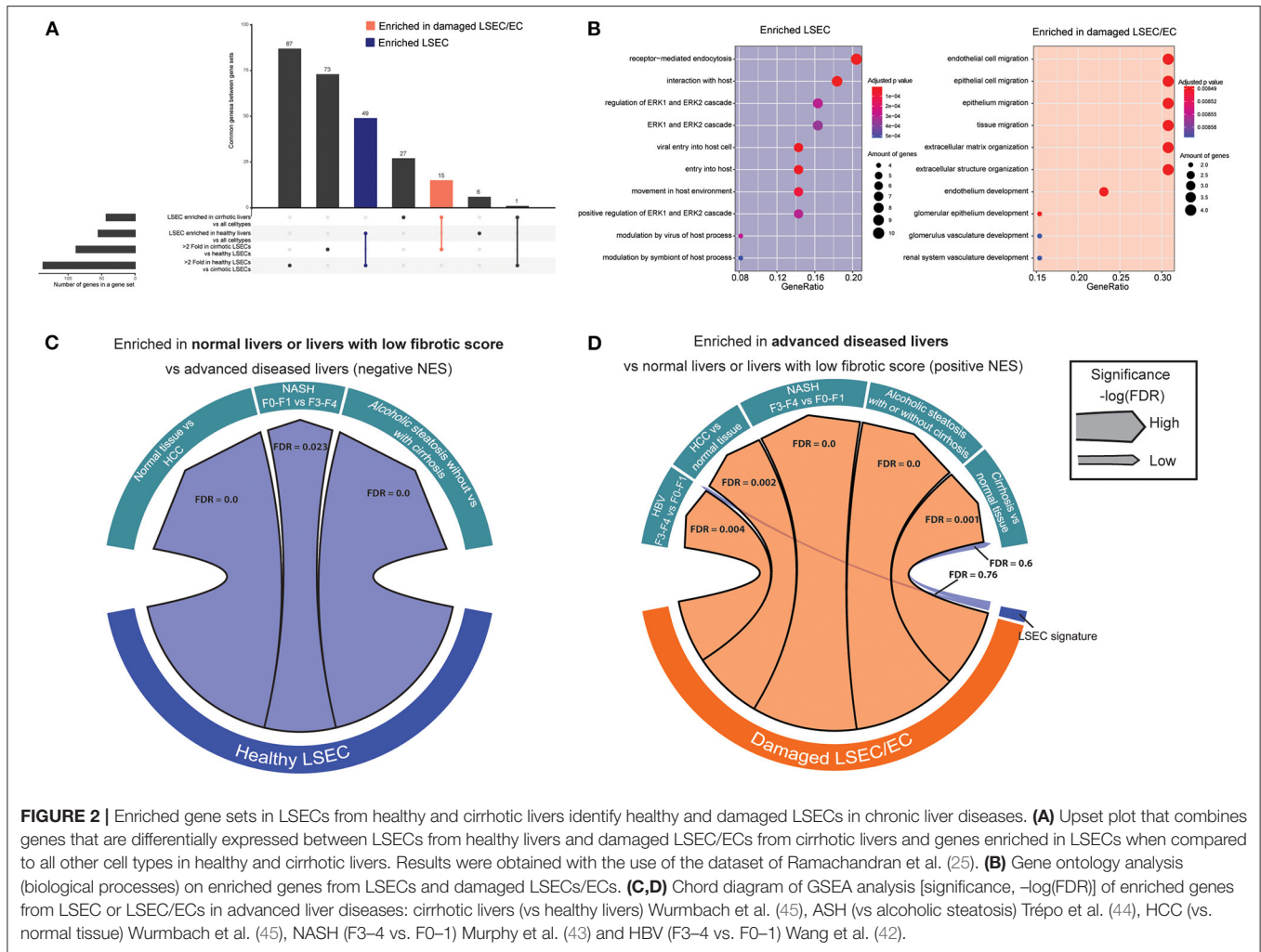
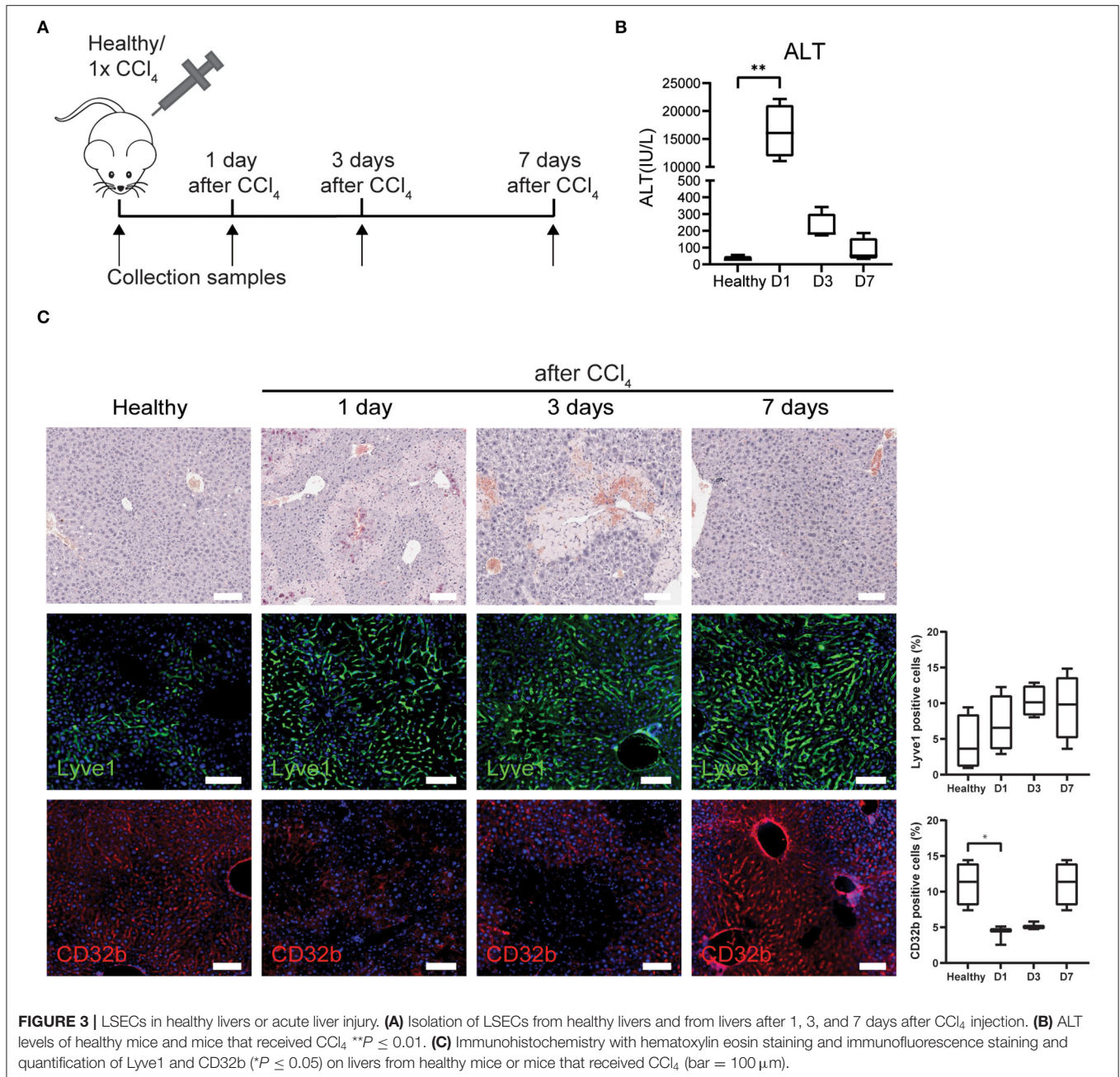


FIGURE 2 | Enriched gene sets in LSECs from healthy and cirrhotic livers identify healthy and damaged LSECs in chronic liver diseases. **(A)** Upset plot that combines genes that are differentially expressed between LSECs from healthy livers and damaged LSEC/ECs from cirrhotic livers and genes enriched in LSECs when compared to all other cell types in healthy and cirrhotic livers. Results were obtained with the use of the dataset of Ramachandran et al. (25). **(B)** Gene ontology analysis (biological processes) on enriched genes from LSECs and damaged LSECs/ECs. **(C,D)** Chord diagram of GSEA analysis [significance, $-\log(\text{FDR})$] of enriched genes from LSEC or LSEC/ECs in advanced liver diseases: cirrhotic livers (vs healthy livers) Wurmbach et al. (45), ASH (vs alcoholic steatosis) Trépo et al. (44), HCC (vs. normal tissue) Wurmbach et al. (45), NASH (F3-4 vs. F0-1) Murphy et al. (43) and HBV (F3-4 vs. F0-1) Wang et al. (42).

LSECs through staining, we see an increased trend of Lyve1 protein levels indicating that LSECs are still present and sinusoids are intact. However, we observed a temporary loss of CD32b expression after 1 and 3 days of CCl₄ treatment, indicating at least partial LSEC dysfunction which is restored after 1 week.

To further analyse LSECs after acute liver injury, livers were collected and LSECs were isolated via FACS at 1, 3, and 7 days after CCl₄ administration (Figure 3A; Supplementary Figure 1B) and transcriptome analysis was performed on the freshly isolated LSECs. Four samples were included for each condition apart from LSECs after 1 day of CCl₄-treatment, because 2 samples did not meet the quality standards for RNA sequencing (low RIN values). Although this reduces the statistical power, still more than 2,000 genes were differentially expressed when compared to healthy LSECs (Supplementary Figure 4). Principal component analysis (PCA) demonstrates separated clusters for each timepoint indicating a change in LSEC transcriptome after exposure to CCl₄ (Figure 4A). Interestingly, LSECs appear not to restore to the healthy LSEC cluster after CCl₄ induced injury, indicating that

LSECs after 1 week CCl₄ have a different phenotype compared to healthy LSECs. Next, pathway analysis was performed on LSECs from CCl₄-treated livers compared to healthy LSECs (40). All enriched pathways were clustered in Cytoscape (Supplementary Figure 5) and graphically represented in Figure 4B. Shortly after the induction of acute liver injury, several pathways related to ROBO signaling and inflammation become significantly enriched (NES > 1, FDR < 0.25). After 3 days, pathways involved in angiogenesis, ECM (extra cellular matrix) production and cell cycle are induced. Interestingly, a considerable amount of cell cycle pathways are strongly active after 3 days of CCl₄ but seem to become inactive again after 7 days. This was confirmed by the presence of Ki67⁺ Lyve1⁺ positive LSECs in livers 3 days after CCl₄, indicating that indeed LSECs are proliferating at day 3, but not anymore after 7 days (Figure 4C). Pathways regarding ECM production were elevated after 3 days of CCl₄ and remained elevated after 7 days. NCAM signaling, important for the inhibition of fibroblast growth factor signaling (51), shows a similar trend. One of the dysregulated ECM genes is Collagen 4 which has been described to be produced by LSECs (52-54). Upon acute injury we indeed see

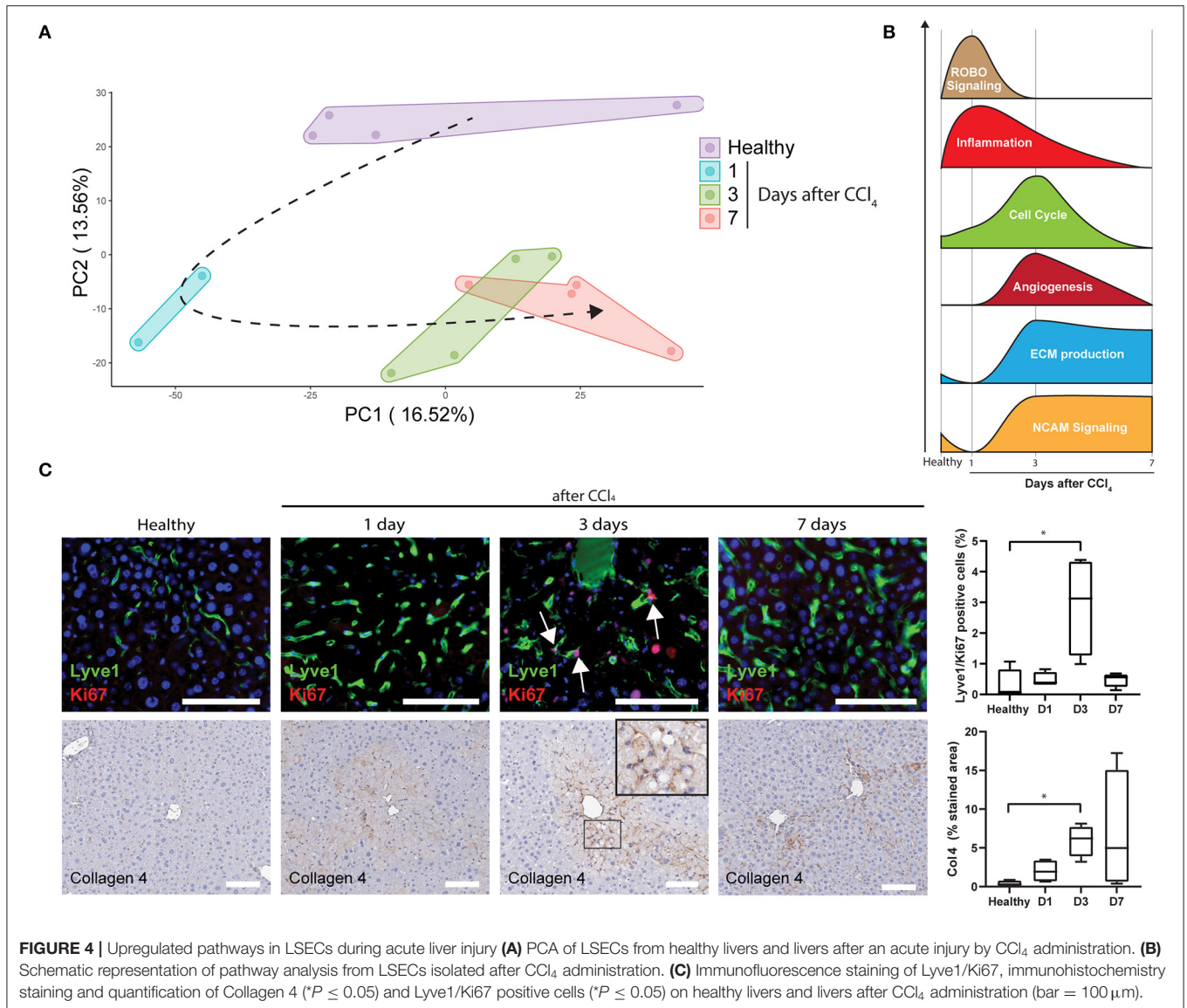


an induction of Collagen 4 expression on day 3, which shows a sinusoidal pattern (Figure 4C).

Generation and Validation of an LSEC- and a Damaged LSEC Signature

To compare human with mouse LSEC dysfunction, we analyzed the expression of human LSEC gene sets (Figures 1, 2) in mouse LSECs after an acute CCl₄-induced liver injury. Genes that are enriched in healthy human LSECs show diverse expression patterns in mouse LSECs after acute liver injury (Figure 5A). Typical LSEC genes such as *STAB2* and *CLEC4G* are downregulated upon liver injury, in contrast to genes

such as *LYVE1*, *CLEC1B*, and *CD36* which are upregulated at early timepoints, indicating that these genes cannot always discriminate healthy LSECs from damaged LSECs. Genes that were expressed higher in healthy LSECs were selected for the generation of a restricted healthy LSEC signature that should identify healthy LSECs in mice and human samples. This signature contains both novel (*PLPP3*, *NTN4* and *OIT3*) and well-established (*CLEC4G* and *STAB2*) genes for LSECs which show a high expression in healthy human LSECs (Figure 5B). To generate also a more restricted gene signature that can specifically identify LSECs in damaged livers instead of both damaged LSECs and ECs, we first identified genes that were differentially



expressed in the damaged LSEC population in comparison to healthy endothelial cells (Figure 5C). These differentially expressed genes were compared to previously identified enriched gene sets from damaged LSECs/ECs (Figure 2A) which resulted in a damaged LSEC signature that contained only four genes: *Fabp4/5* and *Vwf/a1* (Figure 5D). These four genes were all upregulated in CCl₄-induced liver injury after 1 day or 3 days. Moreover, these four genes are highly expressed in the damaged human LSEC population of the Ramachandran et al. (25) data set (Figure 5E). The expression of two healthy and damaged LSEC signature genes were validated using qPCR and confirmed the RNAseq data (Supplementary Figure 2A).

Next, we wanted to examine if scRNAseq data sets of LSECs from healthy and diseased livers can be identified as such with these two LSEC signatures. As samples can differ quite a lot between studies due to a different definition of healthy subjects, different isolation methods, different scRNAseq approaches,

different etiologies and species we validated our newly generated LSECs signatures in 4 independent scRNAseq data sets of healthy human livers (21, 24) and healthy or diseased (NASH and fibrotic) mouse livers (26, 32) (Supplementary Figure 6). Using the LSEC signature we could show a higher gene signature score in LSEC-related populations in healthy human livers compared to all other cell populations (Figures 6A,B). Moreover, the damaged LSEC signature shows a low gene signature score in all liver cell types in healthy human livers except for a slightly higher gene signature score for periportal LSECs and (portal) ECs. These results confirm that quantification of LSEC signatures (scores) can be used to identify LSECs in scRNAseq data of human healthy livers. Unfortunately, we could not validate our signatures in a different scRNAseq data set of cirrhotic patients due to the lack of publicly available human data. Next, we validated the LSEC signatures using scRNAseq data of healthy and diseased (NASH and fibrotic) mouse livers

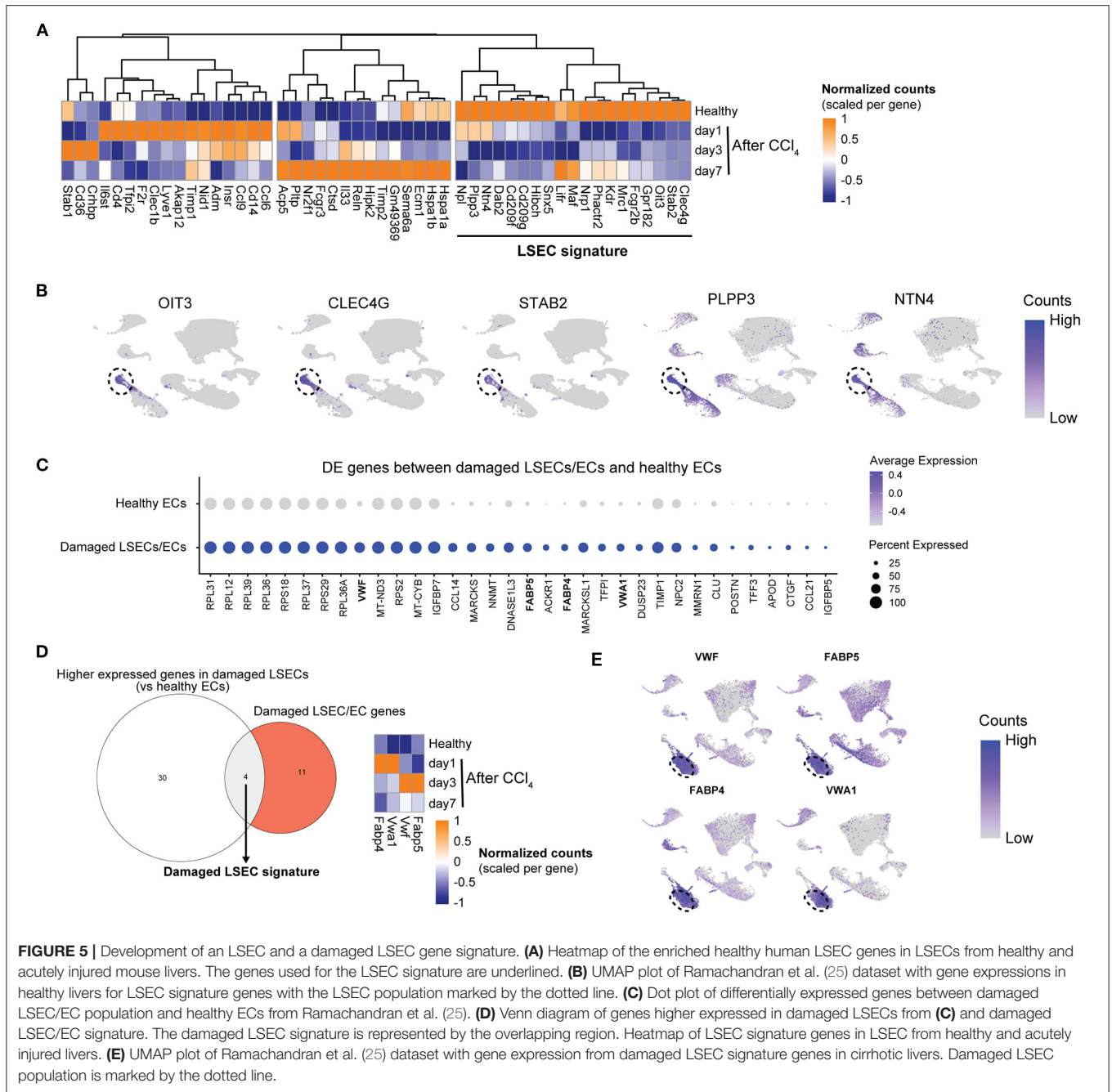


FIGURE 5 | Development of an LSEC and a damaged LSEC gene signature. **(A)** Heatmap of the enriched healthy human LSEC genes in LSECs from healthy and acutely injured mouse livers. The genes used for the LSEC signature are underlined. **(B)** UMAP plot of Ramachandran et al. (25) dataset with gene expressions in healthy livers for LSEC signature genes with the LSEC population marked by the dotted line. **(C)** Dot plot of differentially expressed genes between damaged LSEC/EC population and healthy ECs from Ramachandran et al. (25). **(D)** Venn diagram of genes higher expressed in damaged LSECs from **(C)** and damaged LSEC/EC signature. The damaged LSEC signature is represented by the overlapping region. Heatmap of LSEC signature genes in LSEC from healthy and acutely injured livers. **(E)** UMAP plot of Ramachandran et al. (25) dataset with gene expression from damaged LSEC signature genes in cirrhotic livers. Damaged LSEC population is marked by the dotted line.

(26, 32). In both data sets, the LSEC/EC populations from control livers have a high LSEC signature score, but is also still present (but lower) in NASH and fibrotic livers. More importantly, the damaged LSEC signature score is higher in LSEC/EC population from NASH livers, and to a lesser extent in CCl₄ livers, indicating that LSECs are damaged and can be identified in NASH and fibrotic livers using these 4 genes (**Figures 6C,D**). These findings demonstrate that the LSEC signatures can be used to identify and distinguish damaged LSECs from healthy LSECs in scRNAseq data of human and mouse livers.

DISCUSSION

LSECs are important for liver homeostasis and play a pivotal role in both acute and chronic liver injury by influencing HSCs and other cell types in the liver. scRNAseq studies identified numerous EC populations and revealed well-established and novel LSEC markers for LSECs in healthy and disease states. However, most studies use one specific mouse model (12, 26, 32) or only human cirrhotic livers (25). In this study we sought to generate LSEC signatures that can identify healthy and damaged LSEC populations in multiple transcriptome data sets. We first

focussed on genes enriched in LSEC or damaged LSEC/EC in the human liver scRNAseq data of Ramachandran et al. (25). Using these enriched human gene sets we could show that in cirrhotic livers of patients suffering from HBV, HCC, ASH, and NASH there is a clear enrichment of damaged LSECs. Subsequently, we showed that during acute liver injury in mice certain LSEC specific genes are quickly downregulated which resulted in a more specific LSEC signature that can identify healthy LSECs in mouse and human scRNAseq data. Finally, we developed a damaged LSEC signature comprised of *Fabp4/5* and *Vwf/a1* that can identify damaged LSECs in transcriptome data of NASH and fibrotic mouse livers.

In this study we used CCl_4 to induce an acute liver injury and to evaluate whether the transcriptional changes that occur in LSECs in chronic liver disease already occur upon acute liver damage. After an acute liver injury we observed that LSECs quickly change their phenotype by upregulating *Lyve1*, by temporarily downregulating *CD32b*, proliferating and upregulating ECM genes after 3 days of CCl_4 . Previous studies showed that LSECs can produce a basement membrane during chronic liver injury by deposition of Collagen 4 and Laminin (52, 53, 55). Interestingly, in the data of Ramachandran et al. (25), we also see the expression of *COL4A1* and *COL4A2* mainly in the damaged LSEC/EC population (**Supplementary Figure 7**) indicating that primarily LSECs express *COL4A1* and *COL4A2* in chronically injured human livers. Here, we could show that Collagen 4 deposition is already initiated during acute liver injury.

Here we defined an LSEC signature that contains several well-established LSEC markers such as the scavenger receptors *STAB2*, *CLEC4G*, *CD209*, *MRC1*, and *CD32B* (*Fcgr2b*) but also receptors important for VEGF signaling such as *KDR* and *NRP1* (**Figure 5**). The expression of some of these markers (*STAB2* and *CLEC4G*) has been shown to decrease during chronic liver disease (47). Other genes in this signature are less known but have been mentioned mainly in gene profiling studies (*OIT3*, *NPL*) (24, 56, 57). Genes that showed a higher expression after acute liver injury in mice were not included in the LSEC signature, such as *LYVE1* and *STAB1*. However, we would like to note that these genes could still be useful markers because the induction is scaled per gene, meaning that there is an induction of expression but this induction could be insignificant if the expression of that certain gene is already very high in the LSEC population. There were several other LSEC enriched genes, such as *CLEC1B*, *CD14*, *IL33*, and *CCL6/9*, that showed an induction after acute liver injury and that have been mentioned in other gene profiling studies. This indicates that inflammation could play a role in LSECs during acute liver injury. *TIMP1* and *TIMP2*, often associated with HSCs, also show an induction. Further analysis of these genes in data from Ramachandran et al. (25) showed a strong expression of *TIMP1* and *TIMP2* in LSECs and endothelial cells from human livers indeed showing that these cells do express *TIMP1* and *TIMP2* (**Supplementary Figure 8**). However, *TIMP1* and 2 were not expressed in LSECs or endothelial cells from scRNAseq data from Xiong et al. (26). The damaged LSEC signature contains the known capillarization marker *VWF*, and genes *VWA1*, *FABP4*, and *FABP5*. Further investigation of the

literature shows that protein expression of these signature genes are indeed associated with a damaged LSEC phenotype in mice and human. For example, *FABP4*, also known as (adipocyte) fatty acid binding protein 4, was recently found to be upregulated in LSECs during liver fibrosis, can promote LSEC capillarization and is suggested to be a key regulator involved in the onset and progression of fibrosis in two liver fibrosis models in mice (58). In addition, *FABP4* is also overexpressed in patients with HCC (59). Multiple studies have shown that *vWF* is not expressed by LSECs in healthy livers but is increased in LSECs during fibrosis in several animal models, for example after CCl_4 treatment in mice and rats (60, 61), and NASH with or without cirrhosis in rats (62). Moreover, *vWf*⁺ LSECs were significantly correlated to the fibrosis stage in patients with cirrhosis (63) and a higher *vWF* expression has been linked to old age and pseudocapillarization (64). Targeting LSECs to alleviate fibrosis through one of these 4 genes could be an option as it was recently shown that the treatment with the *FABP4* selective inhibitor BMS309403 alleviated lipopolysaccharide induce acute liver injury and high fat diet-induced NASH in mice (65), and a knockout of *FABP4* reduces fibrosis in CCl_4 and bile duct ligation model in mice (58).

The use of microarray or bulk-seq profiling data can mask the fact that the gene expression signal detected represents only a small portion of a total LSEC population. Few dedifferentiated or damaged LSECs could be responsible for the enrichment of the damaged LSEC/EC gene sets. To obtain more insight into the abundance of dysfunctional LSECs in human and (damaged) mouse livers, more specific LSEC gene signatures were validated in scRNAseq datasets. In this study scRNAseq datasets of different liver disease models were used; two healthy human scRNAseq data sets (21, 24) and two mouse healthy and NASH/fibrotic data sets (26, 32). The recent dataset from Su et al. (12) was not included due to a potential contamination of duplets, making incorporation of this dataset in this study problematic (data not shown). In healthy human livers, the LSEC signature separates LSECs from other liver cells, and only a low signature score is present for periportal LSECs and portal ECs when the damaged LSEC signature is used. Nevertheless, it remains difficult to separate portal and central endothelial cells from portal and central LSECs as they cluster strongly together because LSECs still express endothelial markers such as *CD31* or *CD105* even though these markers have been reported to be lower in LSECs (11, 12). In both healthy and NASH/fibrotic mouse livers, the LSEC signature was abundantly expressed even though the gene signature score is clearly lower in NASH/fibrotic livers which suggests that LSECs partly lose their phenotype in chronic liver disease. More importantly, the damaged LSEC signature had clearly a high gene signature score in all cells of the LSEC/EC population of NASH livers which indicates that all LSECs are damaged in NASH/fibrotic mouse livers. Further scRNAseq analysis of acutely injured mice or human livers would shed more light on the independent changes of different endothelial and LSEC populations and could give more insight into early mechanisms of LSEC-dysfunction or capillarization. A next step in this research could be a larger prospective sequencing effort on biopsy material of livers at different stages of chronic liver disease, or recovering from liver disease, to evaluate whether

one can correlate the rise of a healthy LSEC signature to the improvement of liver fibrosis while a certain level of the damaged LSEC signature can predict progression of the liver disease. Some proteins from the damaged signature could be measured in blood and correlated to the development of fibrosis. For example FABP4 in the blood is already positively correlated to the fibrosis stage and inflammatory grade in patients with NAFLD and NASH (66). In addition, protein levels of the damaged LSEC signature genes could serve as biomarkers for the extent of LSEC damage in acute liver injury, as LSEC damage occurs in ischemia-reperfusion, drug-induced liver injury and hepatic sinusoidal obstruction syndrome (67). For instance, one study showed that FABP4 was elevated in the serum of mice with acute liver injury induced by a single injection of LPS (65). Moreover, in patients with acute liver injury and acute liver failure, vWF is elevated in the serum, but could not be correlated to poor disease outcome (68). One should note that in this study vWF levels could have been affected as blood samples were also collected after NAC administration.

To conclude, we showed that the transcriptome of LSECs transform into a cirrhotic transcriptome independent of the etiology in multiple microarray datasets from human livers. In addition, two unique LSEC signatures were developed and validated in several independent scRNAseq datasets, demonstrating that these signatures can recognize LSECs in healthy and chronically injured livers. Moreover, using several scRNAseq data sets we showed that all LSECs isolated from NASH/fibrotic mouse livers have a damaged LSEC expression profile. These results indicate that during mouse and human chronic liver disease, the change of LSECs toward a cirrhotic dysfunctional phenotype is strong and highlights the potential of LSECs as a therapeutic target for chronic liver disease.

DATA AVAILABILITY STATEMENT

The datasets presented in this study can be found in online repositories. The names of the repository/repositories and accession number(s) can be found in the article.

REFERENCES

1. Wisse E. An electron microscopic study of the fenestrated endothelial lining of rat liver sinusoids. *J Ultrastruct Res.* (1970) 31:125–50. doi: 10.1016/S0022-5320(70)90150-4
2. DeLeve LD. Vascular liver disease and the liver sinusoidal endothelial cell. In: DeLeve LD, Garcia-Tsao G, editors. *Vascular Liver Disease: Mechanisms and Management*. New York, NY: Springer New York (2011). p. 25–40. doi: 10.1007/978-1-4419-8327-5_2
3. Le Couteur DG, Fraser R, Kilmer S, Rivory LP, McLean AJ. The hepatic sinusoid in aging and cirrhosis. *Clin Pharmacokinet.* (2005) 44:187–200. doi: 10.2165/00003088-200544020-00004
4. Mohamad M, Mitchell SJ, Wu LE, White MY, Cordwell SJ, Mach J, et al. Ultrastructure of the liver microcirculation influences hepatic and systemic insulin activity and provides a mechanism for age-related insulin resistance. *Aging Cell.* (2016) 15:706–15. doi: 10.1111/acel.12481
5. Shahani T, Covens K, Lavend'homme R, Jazouli N, Sokal E, Peerlinck K, et al. Human liver sinusoidal endothelial cells but not hepatocytes contain factor VIII. *J Thromb Haemost.* (2014) 12:36–42. doi: 10.1111/jth.12412
6. Lohse AW, Knolle PA, Bilo K, Uhrig A, Waldmann C, Ibe M, et al. Antigen-presenting function and B7 expression of murine sinusoidal endothelial cells and Kupffer cells. *Gastroenterology.* (1996) 110:1175–81. doi: 10.1053/gast.1996.v110.pm8613007
7. Caparrós E, Juanola O, Gómez-Hurtado I, Puig-Kroger A, Piñero P, Zapater P, et al. Liver sinusoidal endothelial cells contribute to hepatic antigen-presenting cell function and Th17 expansion in cirrhosis. *Cells.* (2020) 9:1227. doi: 10.3390/cells9051227
8. Mates JM, Yao Z, Cheplowitz AM, Suer O, Phillips GS, Kwiek JJ, et al. Mouse liver sinusoidal endothelium eliminates HIV-like particles from blood at a rate of 100 million per minute by a second-order kinetic process. *Front Immunol.* (2017) 8:35. doi: 10.3389/fimmu.2017.00035
9. Li R, Oteiza A, Sørensen KK, McCourt P, Olsen R, Smedsrød B, et al. Role of liver sinusoidal endothelial cells and stabilins in elimination of oxidized low-density lipoproteins. *Am J Physiol Gastrointest Liver Physiol.* (2011) 300:G71–81. doi: 10.1152/ajpgi.00215.2010

ETHICS STATEMENT

The animal study was reviewed and approved by Ethical Committee of Animal Experimentation of the Vrije Universiteit Brussel.

AUTHOR CONTRIBUTIONS

SV and EO: conceptualization, investigation, methodology, formal analysis, validation, visualization, data curation, and writing—original draft. VD: investigation and formal analysis. NE: methodology and formal analysis. IM: investigation and methodology. LG: conceptualization, funding acquisition, data curation, and writing—review and editing. All authors contributed to the article and approved the submitted version.

FUNDING

SV was supported by Fund of Scientific Research Flanders (FWO–V) junior post-doctoral fellowship (1243121N). EO was supported by Wetenschappelijk Fonds Willy Gepts of the UZ Brussel (WFWG20-23). VD was supported by FWO 1192920N. IM was supported by FWO–V senior post-doctoral fellowship 12N5419N. The work was also supported by grants awarded to LG European Union's Horizon 2020 research and innovation program under the Marie Skłodowska-Curie Grant Agreement No. 766181, project DeLIVER and FWO-V (G030616 N, G042719 N).

ACKNOWLEDGMENTS

We would like to thank Jean Marc Lazou for performing flow cytometry cell sorting.

SUPPLEMENTARY MATERIAL

The Supplementary Material for this article can be found online at: <https://www.frontiersin.org/articles/10.3389/fmed.2021.750044/full#supplementary-material>

10. Smedsrød B. Clearance function of scavenger endothelial cells. *Comparat Hepatol.* (2004) 3(Suppl. 1):S22. doi: 10.1186/1476-5926-2-S1-S22
11. Strauss O, Phillips A, Ruggiero K, Bartlett A, Dunbar PR. Immunofluorescence identifies distinct subsets of endothelial cells in the human liver. *Sci Rep.* (2017) 7:44356. doi: 10.1038/srep44356
12. Su T, Yang Y, Lai S, Jeong J, Jung Y, McConnell M, et al. Single-cell transcriptomics reveals zone-specific alterations of liver sinusoidal endothelial cells in cirrhosis. *Cell Mol Gastroenterol Hepatol.* (2021) 11:1139–61. doi: 10.1016/j.jcmgh.2020.12.007
13. Poisson J, Lemoine S, Boulanger C, Durand F, Moreau R, Valla D, et al. Liver sinusoidal endothelial cells: physiology and role in liver diseases. *J Hepatol.* (2017) 66:212–27. doi: 10.1016/j.jhep.2016.07.009
14. DeLeve LD, Wang X, Kanel GC, Atkinson RD, McCuskey RS. Prevention of hepatic fibrosis in a murine model of metabolic syndrome with nonalcoholic steatohepatitis. *Am J Pathol.* (2008) 173:993–1001. doi: 10.2353/ajpath.2008.070720
15. Xu B, Broome U, Uzunel M, Nava S, Ge X, Kumagai-Braesch M, et al. Capillarization of hepatic sinusoid by liver endothelial cell-reactive autoantibodies in patients with cirrhosis and chronic hepatitis. *Am J Pathol.* (2003) 163:1275–89. doi: 10.1016/S0002-9440(10)63487-6
16. Warren A, Bertolino P, Benseler V, Fraser R, McCaughan GW, Le Couteur DG. Marked changes of the hepatic sinusoid in a transgenic mouse model of acute immune-mediated hepatitis. *J Hepatol.* (2007) 46:239–46. doi: 10.1016/j.jhep.2006.08.022
17. Ding BS, Cao Z, Lis R, Nolan DJ, Guo P, Simons M, et al. Divergent angiocrine signals from vascular niche balance liver regeneration and fibrosis. *Nature.* (2014) 505:97–102. doi: 10.1038/nature12681
18. Xie G, Wang X, Wang L, Wang L, Atkinson RD, Kanel GC, et al. Role of differentiation of liver sinusoidal endothelial cells in progression and regression of hepatic fibrosis in rats. *Gastroenterology.* (2012) 142:918–27.e6. doi: 10.1053/j.gastro.2011.12.017
19. Elvevold K, Smedsrød B, Martinez I. The liver sinusoidal endothelial cell: a cell type of controversial and confusing identity. *Am J Physiol Gastrointest Liver Physiol.* (2008) 294:G391–400. doi: 10.1152/ajpgi.00167.2007
20. Mousavi SA, Sporstøl M, Fladeby C, Kjekken R, Barois N, Berg T. Receptor-mediated endocytosis of immune complexes in rat liver sinusoidal endothelial cells is mediated by FcγRIIb2. *Hepatology.* (2007) 46:871–84. doi: 10.1002/hep.21748
21. Aizarani N, Saviano A, Sagar, Mailly L, Durand S, Herman JS, et al. A human liver cell atlas reveals heterogeneity and epithelial progenitors. *Nature.* (2019) 572:199–204. doi: 10.1038/s41586-019-1373-2
22. Mouta Carreira C, Nasser SM, di Tomaso E, Padera TP, Boucher Y, Tomarev SI, et al. LYVE-1 is not restricted to the lymph vessels: expression in normal liver blood sinusoids and down-regulation in human liver cancer and cirrhosis. *Cancer Res.* (2001) 61:8079–84.
23. McCourt PA, Smedsrød BH, Melkko J, Johansson S. Characterization of a hyaluronan receptor on rat sinusoidal liver endothelial cells and its functional relationship to scavenger receptors. *Hepatology.* (1999) 30:1276–86. doi: 10.1002/hep.510300521
24. MacParland SA, Liu JC, Ma X-Z, Innes BT, Bartzak AM, Gage BK, et al. Single cell RNA sequencing of human liver reveals distinct intrahepatic macrophage populations. *Nat Commun.* (2018) 9:4383. doi: 10.1038/s41467-018-06318-7
25. Ramachandran P, Dobie R, Wilson-Kanamori JR, Dora EF, Henderson BEP, Luu NT, et al. Resolving the fibrotic niche of human liver cirrhosis at single-cell level. *Nature.* (2019) 575:512–8. doi: 10.1038/s41586-019-1631-3
26. Xiong X, Kuang H, Ansari S, Liu T, Gong J, Wang S, et al. Landscape of intercellular crosstalk in healthy and NASH liver revealed by single-cell secretome gene analysis. *Mol Cell.* (2019) 75:644–60.e5. doi: 10.1016/j.molcel.2019.07.028
27. Stradiot L, Verhulst S, Roosens T, Oie CI, Moya IM, Halder G, et al. Functionality based method for simultaneous isolation of rodent hepatic sinusoidal cells. *Biomaterials.* (2017) 139:91–101. doi: 10.1016/j.biomaterials.2017.05.047
28. Bhandari S, Li R, Simón-Santamaría J, McCourt P, Johansen SD, Smedsrød B, et al. Transcriptome and proteome profiling reveal complementary scavenger and immune features of rat liver sinusoidal endothelial cells and liver macrophages. *BMC Mol Cell Biol.* (2020) 21:85. doi: 10.1186/s12860-020-00331-9
29. Manicardi N, Fernández-Iglesias A, Abad-Jordá L, Royo F, Azkargorta M, Ortega-Ribera M, et al. Transcriptomic profiling of the liver sinusoidal endothelium during cirrhosis reveals stage-specific secretory signature. *Cancers.* (2021) 13:2688. doi: 10.3390/cancers13112688
30. Inverso D, Shi J, Lee KH, Jakab M, Ben-Moshe S, Kulkarni SR, et al. A spatial vascular transcriptomic, proteomic, and phosphoproteomic atlas unveils an angiocrine Tie–Wnt signaling axis in the liver. *Dev Cell.* (2021) 56:1677–93.e10. doi: 10.1016/j.devcel.2021.05.001
31. Stritt M, Stalder AK, Vezzali E. Orbit image analysis: an open-source whole slide image analysis tool. *PLoS Comput Biol.* (2020) 16:e1007313. doi: 10.1371/journal.pcbi.1007313
32. Terkelsen MK, Bendixen SM, Hansen D, Scott EAH, Moeller AF, Nielsen R, et al. Transcriptional dynamics of hepatic sinusoid-associated cells after liver injury. *Hepatology.* (2020) 72:2119–33. doi: 10.1002/hep.31215
33. Hao Y, Hao S, Andersen-Nissen E, Mauck III WM, Zheng S, Butler A, et al. Integrated analysis of multimodal single-cell data. *Cell.* (2021) 184:3573–87. doi: 10.1101/2020.10.12.335331
34. Chen S, Huang T, Zhou Y, Han Y, Xu M, Gu J. AfterQC: automatic filtering, trimming, error removing and quality control for fastq data. *BMC Bioinformatics.* (2017) 18:80. doi: 10.1186/s12859-017-1469-3
35. Dobin A, Davis CA, Schlesinger F, Drenkow J, Zaleski C, Jha S, et al. STAR: ultrafast universal RNA-seq aligner. *Bioinformatics.* (2013) 29:15–21. doi: 10.1093/bioinformatics/bts635
36. Love MI, Huber W, Anders S. Moderated estimation of fold change and dispersion for RNA-seq data with DESeq2. *Genome Biol.* (2014) 15:550. doi: 10.1186/s13059-014-0550-8
37. Carvalho BS, Irizarry RA. A framework for oligonucleotide microarray preprocessing. *Bioinformatics.* (2010) 26:2363–7. doi: 10.1093/bioinformatics/btq431
38. Gautier L, Cope L, Bolstad BM, Irizarry RA. affy—analysis of Affymetrix GeneChip data at the probe level. *Bioinformatics.* (2004) 20:307–15. doi: 10.1093/bioinformatics/btg405
39. Subramanian A, Tamayo P, Mootha VK, Mukherjee S, Ebert BL, Gillette MA, et al. Gene set enrichment analysis: a knowledge-based approach for interpreting genome-wide expression profiles. *Proc Natl. Acad Sci USA.* (2005) 102:15545–50. doi: 10.1073/pnas.0506580102
40. Shannon P, Markiel A, Ozier O, Baliga NS, Wang JT, Ramage D, et al. Cytoscape: a software environment for integrated models of biomolecular interaction networks. *Genome Res.* (2003) 13:2498–504. doi: 10.1101/gr.1239303
41. Reimand J, Isserlin R, Voisin V, Kucera M, Tannus-Lopes C, Rostamianfar A, et al. Pathway enrichment analysis and visualization of omics data using g:Profiler, GSEA, Cytoscape and EnrichmentMap. *Nat Protoc.* (2019) 14:482–517. doi: 10.1038/s41596-018-0103-9
42. Wang M, Gong Q, Zhang J, Chen L, Zhang Z, Lu L, et al. Characterization of gene expression profiles in HBV-related liver fibrosis patients and identification of ITGBL1 as a key regulator of fibrogenesis. *Sci Rep.* (2017) 7:43446. doi: 10.1038/srep43446
43. Murphy SK, Yang H, Moylan CA, Pang H, Dellinger A, Abdelmalek MF, et al. Relationship between methylome and transcriptome in patients with nonalcoholic fatty liver disease. *Gastroenterology.* (2013) 145:1076–87. doi: 10.1053/j.gastro.2013.07.047
44. Trépo E, Goossens N, Fujiwara N, Song WM, Colaprico A, Marot A, et al. Combination of gene expression signature and model for end-stage liver disease score predicts survival of patients with severe alcoholic hepatitis. *Gastroenterology.* (2018) 154:965–75. doi: 10.1053/j.gastro.2017.10.048
45. Wurmbach E, Chen YB, Khitrov G, Zhang W, Roayaie S, Schwartz M, et al. Genome-wide molecular profiles of HCV-induced dysplasia and hepatocellular carcinoma. *Hepatology.* (2007) 45:938–47. doi: 10.1002/hep.21622
46. Lozach P-Y, Amara A, Bartosch B, Virelizier J-L, Arenzana-Seisdedos F, Cosset F-L, et al. C-type Lectins L-SIGN and DC-SIGN capture and transmit infectious hepatitis C virus pseudotype particles*. *J Biol Chem.* (2004) 279:32035–45. doi: 10.1074/jbc.M402296200

47. Pandey E, Nour AS, Harris EN. Prominent receptors of liver sinusoidal endothelial cells in liver homeostasis and disease. *Front Physiol.* (2020) 11:873. doi: 10.3389/fphys.2020.00873
48. Thabut D, Shah V. Intrahepatic angiogenesis and sinusoidal remodeling in chronic liver disease: new targets for the treatment of portal hypertension? *J Hepatol.* (2010) 53:976–80. doi: 10.1016/j.jhep.2010.07.004
49. Coulon S, Heindryckx F, Geerts A, Van Steenkiste C, Colle I, Van Vlierberghe H. Angiogenesis in chronic liver disease and its complications. *Liver Int.* (2011) 31:146–62. doi: 10.1111/j.1478-3231.2010.02369.x
50. Mootha VK, Lindgren CM, Eriksson K-F, Subramanian A, Sihag S, Lehar J, et al. PGC-1 α -responsive genes involved in oxidative phosphorylation are coordinately downregulated in human diabetes. *Nat Genet.* (2003) 34:267–73. doi: 10.1038/ng1180
51. Cavallaro U, Dejana E. Adhesion molecule signalling: not always a sticky business. *Nat Rev Mol Cell Biol.* (2011) 12:189–97. doi: 10.1038/nrm3068
52. Herbst H, Frey A, Heinrichs O, Milani S, Bechstein WO, Neuhaus P, et al. Heterogeneity of liver cells expressing procollagen types I and IV *in vivo*. *Histochem Cell Biol.* (1997) 107:399–409. doi: 10.1007/s004180050126
53. Hahn E, Wick G, Pencev D, Timpl R. Distribution of basement membrane proteins in normal and fibrotic human liver: collagen type IV, laminin, and fibronectin. *Gut.* (1980) 21:63–71. doi: 10.1136/gut.21.1.63
54. Wells RG. Cellular sources of extracellular matrix in hepatic fibrosis. *Clin Liver Dis.* (2008) 12:759–68. doi: 10.1016/j.cld.2008.07.008
55. de Haan W, Dheedene W, Apelt K, Décombas-Deschamps S, Vinckier S, Verhulst S, et al. Endothelial Zeb2 preserves the hepatic angioarchitecture and protects against liver fibrosis. *Cardiovasc Res.* (2021). doi: 10.1093/cvr/cvab148. [Epub ahead of print].
56. De Smedt J, van Os EA, Talon I, Ghosh S, Toprakchisar B, Furtado Madeiro Da Costa R, et al. PU.1 drives specification of pluripotent stem cell-derived endothelial cells to LSEC-like cells. *Cell Death Dis.* (2021) 12:84. doi: 10.1038/s41419-020-03356-2
57. de Haan W, Øie C, Benkheil M, Dheedene W, Vinckier S, Coppiello G, et al. Unraveling the transcriptional determinants of liver sinusoidal endothelial cell specialization. *Am J Physiol Gastrointest Liver Physiol.* (2020) 318:G803–15. doi: 10.1152/ajpgi.00215.2019
58. Wu X, Shu L, Zhang Z, Li J, Zong J, Cheong LY, et al. Adipocyte fatty acid binding protein promotes the onset and progression of liver fibrosis via mediating the crosstalk between liver sinusoidal endothelial cells and hepatic stellate cells. *Adv Sci.* (2021) 8:2003721. doi: 10.1002/advs.202003721
59. Laouirem S, Sannier A, Norkowski E, Cauchy F, Doblas S, Rautou PE, et al. Endothelial fatty liver binding protein 4: a new targetable mediator in hepatocellular carcinoma related to metabolic syndrome. *Oncogene.* (2019) 38:3033–46. doi: 10.1038/s41388-018-0597-1
60. Wu Y, Li Z, Xiu AY, Meng DX, Wang SN, Zhang CQ. Carvedilol attenuates carbon tetrachloride-induced liver fibrosis and hepatic sinusoidal capillarization in mice. *Drug Des Devel Ther.* (2019) 13:2667–76. doi: 10.2147/DDDT.S210797
61. Zhao S, Zhang Z, Qian L, Lin Q, Zhang C, Shao J, et al. Tetramethylpyrazine attenuates carbon tetrachloride-caused liver injury and fibrogenesis and reduces hepatic angiogenesis in rats. *Biomed Pharmacother.* (2017) 86:521–30. doi: 10.1016/j.biopha.2016.11.122
62. Maeso-Díaz R, Boyer-Díaz Z, Lozano JJ, Ortega-Ribera M, Peralta C, Bosch J, et al. New rat model of advanced NASH mimicking pathophysiological features and transcriptomic signature of the human disease. *Cells.* (2019) 8:1062. doi: 10.3390/cells8091062
63. Arimoto J, Ikura Y, Suekane T, Nakagawa M, Kitabayashi C, Iwasa Y, et al. Expression of LYVE-1 in sinusoidal endothelium is reduced in chronically inflamed human livers. *J Gastroenterol.* (2010) 45:317–25. doi: 10.1007/s00535-009-0152-5
64. Le Couteur DG, Warren A, Cogger VC, Smedsrod B, Sørensen KK, De Cabo R, et al. Old age and the hepatic sinusoid. *Anatomical Rec.* (2008) 291:672–83. doi: 10.1002/ar.20661
65. Hoo RLC, Lee IPC, Zhou M, Wong JYL, Hui X, Xu A, et al. Pharmacological inhibition of adipocyte fatty acid binding protein alleviates both acute liver injury and non-alcoholic steatohepatitis in mice. *J Hepatol.* (2013) 58:358–64. doi: 10.1016/j.jhep.2012.10.022
66. Milner K-L, van der Poorten D, Xu A, Bugianesi E, Kench JG, Lam KSL, et al. Adipocyte fatty acid binding protein levels relate to inflammation and fibrosis in nonalcoholic fatty liver disease. *Hepatology.* (2009) 49:1926–34. doi: 10.1002/hep.22896
67. Gracia-Sancho J, Caparrós E, Fernández-Iglesias A, Francés R. Role of liver sinusoidal endothelial cells in liver diseases. *Nat Rev Gastroenterol Hepatol.* (2021) 18:411–31. doi: 10.1038/s41575-020-00411-3
68. Hugenholtz GC, Adelmeijer J, Meijers JC, Porte RJ, Stravitz RT, Lisman T. An imbalance between von Willebrand factor and ADAMTS13 in acute liver failure: implications for hemostasis and clinical outcome. *Hepatology.* (2013) 58:752–61. doi: 10.1002/hep.26372

Conflict of Interest: The authors declare that the research was conducted in the absence of any commercial or financial relationships that could be construed as a potential conflict of interest.

Publisher's Note: All claims expressed in this article are solely those of the authors and do not necessarily represent those of their affiliated organizations, or those of the publisher, the editors and the reviewers. Any product that may be evaluated in this article, or claim that may be made by its manufacturer, is not guaranteed or endorsed by the publisher.

Copyright © 2021 Verhulst, van Os, De Smet, Eysackers, Mannaerts and van Grunsven. This is an open-access article distributed under the terms of the Creative Commons Attribution License (CC BY). The use, distribution or reproduction in other forums is permitted, provided the original author(s) and the copyright owner(s) are credited and that the original publication in this journal is cited, in accordance with accepted academic practice. No use, distribution or reproduction is permitted which does not comply with these terms.